

Search for multiphoton-induced inner-shell excitations

P. H. Y. Lee, D. E. Casperson, and G. T. Schappert

Los Alamos National Laboratory, Mail Stop E-526, Los Alamos, New Mexico 87545

(Received 16 March 1989)

Photon-counting experiments have been conducted to test the conjecture that at sufficiently high laser irradiance, atomic inner-shell excitations can be induced by laser-driven outer-shell oscillations. Using KrF light at an irradiance $\approx 3 \times 10^{17}$ W/cm² on low-density noble-gas targets, we detect no prompt photons which are characteristic of inner-shell processes.

Recent experiments¹ on the collision-free multiphoton ionization of atoms by intense (10^{15} – 10^{17} W/cm²), short-wavelength, picosecond laser pulses have shown effects of unusually strong nonlinear coupling of the laser energy to the atoms. On this basis Boyer and Rhodes² (BR) have conjectured that atomic inner-shell excitations can be induced by laser-driven coherent oscillation of the outer-shell electrons, provided that the laser irradiance is sufficiently high such that the optical field strength exceeds an atomic unit e/a_0^2 . Although this view is further supported by theoretical modeling,³ Lambropoulos⁴ doubts that a whole atomic shell can be excited; he reasons that even if an excitation channel exists within the appropriate energy range, it must compete with other processes that occur much faster at lower irradiances. Consequently, a neutral atom can never be influenced by the peak laser irradiance. Wendin *et al.*⁵ pointed out that screening by outermost shells in heavy atoms lowers the effective irradiance seen by the inner shell, making it more difficult to create an inner-shell vacancy. Nevertheless, if the BR conjecture were correct, then it would provide a basis for the expectation that stimulated emission of x rays can be produced by direct, highly nonlinear coupling of short-wavelength (uv) radiation to atoms.⁶ Indeed, Biedenharn *et al.*⁷ have suggested that ordered many-electron motion in atoms will offer new possibilities for achieving collisionless nuclear excitation, and experiments are in progress to test this idea by searching for the 73-eV isomeric level of coherently excited ²³⁵U atoms. This laser-atom-nucleus coupling could be an important mechanism for a γ -ray laser scheme.⁸

In order to directly test the idea of whether or not multiphoton processes at very high laser irradiance can induce inner-shell excitation, we have used the Los Alamos Bright Source (LABS) laser to irradiate low-density noble-gas targets at $I > 10^{17}$ W/cm² and have conducted photon-counting experiments to search for “prompt” radiation, i.e., photons characteristic of the relaxation of collisionless inner-shell excitations. In the present context, “inner-shell” means the shells adjacent to the outermost shell. As an example, our data⁹ on multiphoton ionization of Xe atoms indicate that at 10^{17} W/cm², a substantial fraction of the *O* shell can be stripped, the highest measured charge state being Xe¹¹⁺ which re-

quires a cumulative ionization energy (starting from a neutral atom) of ~ 1 keV. The radiation which is characteristic of multiphoton inner-shell excitation would thus be photons in the 90–140-eV range for transitions between the *N* and *O* levels and photons in the 500–1000-eV range for transitions between the *M* and *N* levels. This article reports the results of the photon-counting experiments.

The LABS laser consists of a mode-locked visible dye laser heterodyned to 248 nm and amplified in two KrF amplifiers. Output is typically 20 mJ of 0.7-ps pulses at a repetition rate of 3 Hz. The pulse can be focused, using an $f/1$ parabolic mirror, to a minimum spot size of ~ 5 μm^2 . A detailed description of LABS is published elsewhere.¹⁰ A schematic of the experimental configuration is shown in Fig. 1. Laser pulses from LABS are directed into the target chamber by one or more turning mirrors, while a small fraction of the light passes through the mir-

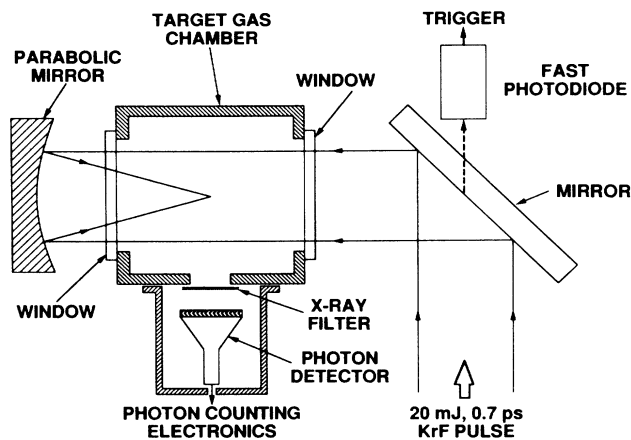


FIG. 1. Schematic of experiment. The vacuum on the detector side is maintained at $\sim 10^{-7}$ Torr while the target chamber gas pressure can be varied between 3×10^{-8} to 0.3 Torr. The thin x-ray filter serves as a vacuum window as well as a uv (5 eV-laser-photons) shield. Photon-counting data are accumulated by a 1024-channel multichannel analyzer with 1-ns resolution.

ror to a fast photodiode providing a trigger for timing reference in the detector electronics. A 50-mm-diam $f/1$ parabolic mirror focuses the beam down to best focus at the center of the target chamber. The target chamber is filled with a given noble gas at low pressure. Average peak irradiance on target, accounting for all measured mirror and target chamber window losses, is $\sim 3 \times 10^{17}$ W/cm²; the optical field strength corresponding to this irradiance is ~ 3 a.u. X-ray photons generated in the focal region (i.e., the laser atom interaction region) are detected through a thin-foil filter by a photon-counting system consisting of either a fast, high-gain microchannel-plate (MCP) detector or a slower, high-gain MCP-phosphor-photomultiplier detector assembly; the detectors subtend a variety of solid angles with respect to the interaction region. Three different filters were used for the experiments: filter 1 consists of 1 μm of parylene (C₈H₈) and 1000 Å of aluminum (500 Å evaporated on each side of the parylene); filter 2 consists of 2 μm of parylene and 2000 Å of aluminum, i.e., filter 1 doubled; filter 3 consists of 5 μm of beryllium. The filter transmissions are plotted in Fig. 2 using the data of Henke *et al.*¹¹

Precise alignment of the focal volume to the correct position is achieved by using an alignment aid—a steel needle, whose tip can be micropositioned to the center of the target chamber. For photon detection, a fiducial at “zero time” is established by measuring the “prompt” x rays generated from a solid target (the needle tip) when irradiated by KrF pulses. A multichannel analyzer with 1-ns resolution provides temporal discrimination between “prompt” (<1-ns delay) and delayed x rays. Spectral discrimination is provided by the set of different thin-foil filters described above. There are two possible mechanisms from which prompt photons may be generated: namely, multiphoton inner-shell excitation leaving excited states which decay by emission of a photon, where the

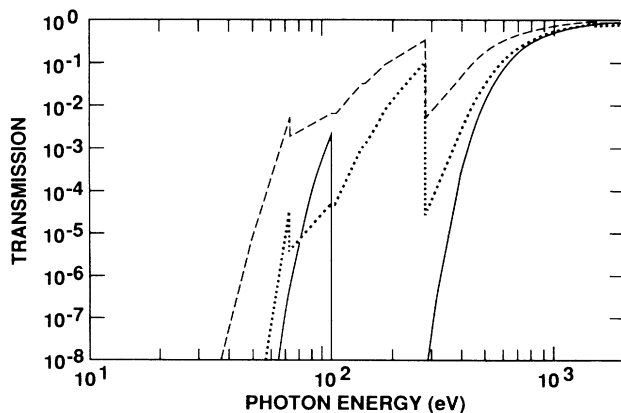


FIG. 2. Transmission of thin-foil filters used in the experiments. Dashed line, filter (1- μm parylene + 0.1- μm aluminum); dotted line, filter 2 (2- μm parylene + 0.2- μm aluminum); solid line, filter 3 (5- μm beryllium). The experimental results indicate that the energy range immediately below the Be K edge (111 eV) is the region where delayed photons are observed.

lifetimes of these states are much less than 1 ns, and bremsstrahlung from the quivering electrons in the vicinity of the parent ion. Since the quiver energy is $E = (e^2/\pi mc^3)I\lambda^2$, peak energies over 1 keV are possible for a KrF laser at $I > 10^{17}$ W/cm². The photons generated by these two mechanisms, i.e., inner-shell radiation versus bremsstrahlung, are, in principle, spectrally distinguishable.

The zero-time fiducial measurement is made each time a new experimental configuration is used, and checked often between experimental runs. A typical 200 shot zero-time fiducial measurement using the fast MCP detector records a count at every shot, giving the following distribution: 61.5% of the total counts occur at the t_0 (prompt) bin, 25% occur at the $(t_0 + 1)$ -ns bin, 0.5% occur at the $(t_0 + 2)$ -ns bin, 9.5% occur at the $(t_0 - 1)$ -ns bin, and 3.5% occur at the $(t_0 - 2)$ -ns bin. A curve fit through this distribution gives a full width at half maximum (FWHM) of 1.4 ns, which is indicative of the temporal resolution of the photon-counting system electronics. The small number of counts scattered around the t_0 bin are attributed to several sources: laser amplified spontaneous emission that lasts for about 10 ns and contains up to a few percent of the laser energy, small errors in focusing the laser beam on the steel needle leading to extended laser-plasma interactions near the surface, and jitter in the detection electronics. Background calibrations of both types of detectors at a variety of solid angles were obtained at a background target-chamber pressure of 1×10^{-7} Torr, for a total of 3.4×10^4 laser shots. The background count rate is found to be 0.3 per 10^3 shots for the fast MCP and less than 0.7 per 10^3 shots for the slower MCP-phosphor-PMT, regardless of filter used.

Four main photon-counting experiments using the fast (FWHM of 1.4 ns) MCP and Xe gas at 0.124 Torr gave the following results.

(1) With the detector subtending a solid angle Ω of 7.85×10^{-3} sr and using filter 1, a 1.2×10^4 -shot run produced a total of 60 counts between the 0- and 1000-ns bins. For this run, the earliest count was recorded at 6 ns after the t_0 fiducial. We note that there are many delayed photons but no prompt ones. The 1000 Å of aluminum on the filter serves as a uv shield; in its absence the detector would record scattered 5-eV laser photons at t_0 from every laser shot.

(2) At $\Omega = 7.85 \times 10^{-3}$ sr with filter 3, a 2.8×10^4 -shot run recorded a total of 69 counts. Again there are delayed photons, with the earliest count recorded at 2 ns after t_0 .

(3) Using filter 1 and changing to a larger solid angle ($\Omega = 2 \times 10^{-2}$ sr), a 1.2×10^4 -shot run recorded 120 counts, with the earliest count occurring at 3 ns after t_0 .

(4) At $\Omega = 2 \times 10^{-2}$ sr with filter 2, a 10^4 -shot run provided only three delayed counts, which, incidentally, is the background-count rate. This means that the delayed photons are practically not transmitted through filter 2.

From the experimental results, we note the following: filter 1 is more transmissive (by more than a factor of 2) than filter 3, while filter 2 is not transmissive. The count rate peaks at ~ 8 ns after t_0 followed by a gradual decay over several hundred nanoseconds. A typical count his-

togram is shown in Fig. 3.

With the null result of prompt photons in experiments 1–3 described above, we can estimate an upper limit for the probability (P) that a prompt x ray will be generated in a Xe atom by either the multiphoton inner-shell excitation or bremsstrahlung mechanism. The number density of Xe atoms at 0.124 Torr is $4.38 \times 10^{15} \text{ cm}^{-3}$ and the focal volume [(focal-spot area) \times (Rayleigh range)] is $\sim 100 \mu\text{m}^3$; hence, there are $N = 4.38 \times 10^5$ atoms in the focal volume. The detector solid angle is $\Omega = 7.85 \times 10^{-3} \text{ sr}$ (we will use the smaller value for a conservative estimate). A filter transmission of $T = 10^{-3}$ is assumed (again being conservative, since P will be smaller if T is larger), and the MCP efficiency for sub-keV photons is $\eta \sim 0.1$. The total number of shots was $N_s = 5.2 \times 10^4$. Folding in all these parameters we arrive at an upper limit for P ,

$$P < (N_s N \Omega T \eta)^{-1} = 5.6 \times 10^{-5}.$$

A sharper estimate of P can be obtained if we consider the earliest single count which occurred at $t_0 + 2 \text{ ns}$ as having a 0.5% probability (recall the distribution for the fiducial) of actually being a “prompt.” We then get $P \leq 2.8 \times 10^{-7}$. In any case, P is negligibly small. The probability of quivering electrons producing bremsstrahlung can be estimated from the thermal bremsstrahlung emission formula,¹²

$$\epsilon = 1.4 \times 10^{-27} \sqrt{T_e} n_e n_i Z^2 g_B \text{ erg s}^{-1} \text{ cm}^{-3},$$

where g_B is a frequency average of the velocity-averaged Gaunt factor. Using reasonably high electron densities

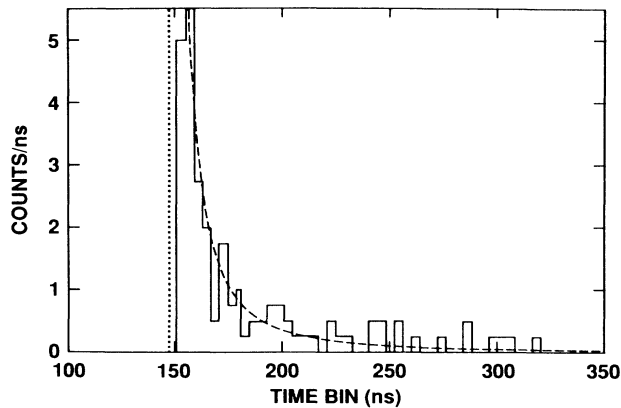


FIG. 3. A typical count histogram displaying channels 100–350. This was recorded from a 1.2×10^4 -shot run with Xe gas at 0.124 Torr using the fast MCP detector at a solid angle of $\Omega = 2 \times 10^{-2} \text{ sr}$ and the compound filter of 1- μm parylene + 1000- \AA aluminum. The dotted line marks the t_0 fiducial, i.e., the time at which prompt x rays should arrive. The earliest count for this run was recorded at 3 ns after t_0 . Common to all the data, no prompt counts were recorded and peak count rate occurred at $\sim 8 \text{ ns}$ after t_0 . Although the multichannel analyzer has 1-ns resolution, this histogram is bin-averaged (4-ns-wide bin) for easier visualization. The model $\text{const}/[1 + (t - t_p)/\tau]^2$, with $\tau \sim 15 \text{ ns}$ gives the best fit (dashed curve) to the “decay” of count rate with respect to time.

($n_e > n_i$), $Z \sim 10$, and an unrealistically large electron temperature (i.e., T_e corresponding to peak electron quiver energy of 1 keV) still yields negligible values of ϵ . Since the filters do not transmit any photons with energy less than $\sim 50 \text{ eV}$, we may say that at $I \sim 3 \times 10^{17} \text{ W/cm}^2$ of KrF light, *there are no measurable prompt photons of energy greater than 50 eV, regardless of the generating mechanism.*

On the other hand, the probability of generating a delayed photon per atom in the focal volume is $\sim 10^{-2}$, as derived from our measurements. The energy of the delayed photons can be determined by noting that filter 1 is more transmissive than filter 3, while filter 2 does not transmit the delayed photons. By examining Fig. 2, we find that such a condition can only be satisfied in the energy range of 80–110 eV. We need to point out, however, that the transmission values of thin foils below $\sim 70 \text{ eV}$ are not well characterized and subject to great uncertainty. In any case, we can conservatively claim that the delayed photons are in the energy range below 110 eV.

Photon-counting experiments using different noble gases and different pressures provide us with data on Z scaling and pressure scaling. It should be obvious that multiphoton inner-shell excitation is much less probable for lower- Z atoms because ionization energies are much higher. Nevertheless, using the larger solid angle ($3.75 \times 10^{-2} \text{ sr}$) MCP-phosphor-PMT detector with a 5- μm Be filter, a 2000-shot run at $\sim 0.125 \text{ Torr}$ produced a total of 26 (delayed) counts for Xe, 11 counts for Kr, 5 counts for Ar, 1 count for Ne, and 0 for He. These Z scaling data, coupling with our measurements on multiphoton ionization,⁹ indicate that the number of delayed photons is correlated to the ion-charge states that are generated: the more abundant and the higher the charge state, the greater the number of delayed photon counts. Pressure scaling indicates that the number of total counts increases with pressure. However, there is a limit to the operating pressure because the thin filter which also serves as a vacuum window for the detector fails to withstand the pressure differential.

From the experimentally derived probability of generating delayed photons from Xe atoms, as well as the Z -scaling results, we believe that delayed photons are generated by recombination with electrons or by charge exchange and subsequent relaxation of the higher charge-state ions (which are created in the innermost portion of the focal volume) with lower charge-state ions and neutral atoms. However, these mechanisms evolve in time with the expansion and cooling of the focal volume, thus the detailed processes are not easily unraveled. In order to model the generation of delayed photons, many additional parameters (e.g., the cross sections for various recombination mechanisms, the exact shape of the interaction region, the initial electron density, the ion species densities and their initial spatial distributions, and the electron and ion temperatures in the focal volume) need to be known. Nonetheless, we provide an additional experimental detail which hopefully will shed some light on this issue. The previously described Experiment 3 which recorded 120 counts provides reasonable statistics for a curve to be fit to the “decaying” portion of the

count histogram. The best fit for the decay rate is obtained not with an exponential which would be expected if charge exchange were the dominant mechanism, but with a curve with the functional form which is characteristic of radiative recombination, i.e., $[1+(t-t_p)/\tau]^{-2}$, where t_p is the time bin of the peak count rate, with $\tau \sim 15$ ns being the value of the best fit (see Fig. 3). However, the rate constant κ derived from using the upper limit of $n_i \leq 4.4 \times 10^{15} \text{ cm}^{-3}$ and the curve-fitted value of τ gives $\kappa \sim (n_i \tau)^{-1} \geq 1.5 \times 10^{-8} \text{ cm}^3/\text{s}$, which is *too large* (by orders of magnitude) compared to computed values of rate constants for radiative recombination in *uniform plasmas*. In another experiment a 10^4 -shot run using the MCP-phosphor-PMT detector at $\Omega = 3.75 \times 10^{-2}$ sr, with the $5 \mu\text{m}$ Be filter and Xe at 0.124 Torr, produced a total of 141 counts. Again the best fit to the "decaying" portion of the histogram is a radiative-recombination-type function, but the rate constant derived from the fit is again too large compared to computed values. This result is therefore repro-

ducible, but at the same time it clearly indicates that the generation of delayed photons is not a simple process. Although the issue of delayed photons is not the theme of this article, the understanding of the process for delayed photon generation warrants further investigation.

In conclusion, based on the results of detecting no prompt photons from 5.2×10^4 laser shots, we believe that the mechanism of inner-shell excitation driven by coherent outer-shell oscillation is *inoperative* at $I \sim 3 \times 10^{17} \text{ W/cm}^2$. Perhaps the mechanism will become effective at *significantly* higher irradiances, but this remains to be seen.

We gratefully acknowledge the contribution of S. Harper, A. Taylor, and J. Roberts for operating LABS; K. Stetler for technical assistance; and L. Jones and Professor H. Griem for useful discussions. This work was performed under the auspices of the U.S. Department of Energy under Contract No. W-740-ENG-36.

¹T. S. Luk, U. Johann, H. Egger, H. Pummer, and C. K. Rhodes, Phys. Rev. A **32**, 214 (1985); U. Johann, T. S. Luk, H. Egger, and C. K. Rhodes, *ibid.* **34**, 1084 (1986).

²K. Boyer and C. K. Rhodes, Phys. Rev. Lett. **54**, 1490 (1985).

³A. Szöke and C. K. Rhodes, Phys. Rev. Lett. **56**, 720 (1986).

⁴P. Lambropoulos, Phys. Rev. Lett. **55**, 2141 (1985).

⁵G. Wendin, L. Jönsson, and A. L'Huillier, Phys. Rev. Lett. **56**, 1241 (1986).

⁶C. K. Rhodes, Science **229**, 1345 (1985); and (unpublished).

⁷L. C. Biedenharn, G. C. Baldwin, K. Boyer, and J. C. Solem in *Advances in Laser Science—I, Proceedings of the First International Laser Science Conference* (AIP Conf. Proc. No. 146) (AIP, New York, 1985), p. 52; G. A. Rinker, J. C. Solem, and L. C. Biedenharn, in *Advances in Laser Science—II, Proceed-*

ings of the First International Laser Science Conference (AIP Conf. Proc. No. 160) (AIP, New York, 1986), p. 75.

⁸P. Dyer, J. A. Bounds, R. C. Haight, and T. S. Luk, Proc. Soc. Photo-Opt. Instrum. Eng. **875**, edited by C. R. Jones (SPIE, Bellingham, Washington, 1988) p. 88.

⁹G. A. Kyrala, D. E. Casperson, P. H. Y. Lee, L. A. Jones, G. T. Schappert, and A. J. Taylor (unpublished).

¹⁰J. P. Roberts, A. J. Taylor, P. H. Y. Lee, and R. B. Gibson, Opt. Lett. **13**, 734 (1988).

¹¹B. Henke, P. Lee, T. J. Tanaka, R. L. Shimabukuro, and B. K. Fujikawa, At. Data Nucl. Data Tables, **27**, 1 (1982).

¹²See, for example, G. B. Rybicki and A. L. Lightman, *Radiative Processes in Astrophysics* (Wiley, New York, 1979) p. 162.